Research Square

Preprints are preliminary reports that have not undergone peer review.
They should not be considered conclusive, used to inform clinical practice,
or referenced by the media as validated information.

# Altered Cortical Complexity and Network Topology in End-Stage Kidney Disease Patients with Mild Cognitive Impairment

**Jing Yang**
First Affiliated Hospital of Xi'an Jiaotong University
**Huijie Yuan**
First Affiliated Hospital of Xi'an Jiaotong University
**Xia Luo**
First Affiliated Hospital of Xi'an Jiaotong University
**Zhaoyao Luo**
First Affiliated Hospital of Xi'an Jiaotong University
**Qiange Zhu**
First Affiliated Hospital of Xi'an Jiaotong University
**Wen Gu**
First Affiliated Hospital of Xi'an Jiaotong University
**Shaohui Ma**
First Affiliated Hospital of Xi'an Jiaotong University
**Peng Li**
First Affiliated Hospital of Xi'an Jiaotong University
**Dun Ding**
Second Affiliated Hospital of Xi'an Jiaotong University
**Xueying Ma**
the Affiliated Hospital of Inner Mongolia Medical University
**Junya Mu**
First Affiliated Hospital of Xi'an Jiaotong University
**Ming Zhang**
zhangming01@xjtu.edu.cn

First Affiliated Hospital of Xi'an Jiaotong University

---

**Research Article**

**Keywords:** End-stage kidney disease, Mild cognitive impairment, Magnetic resonance imaging, Surface-based morphometry, Structural covariance network

**Posted Date:** June 18th, 2026

**DOI:** https://doi.org/10.21203/rs.3.rs-9792022/v1

**License:** This work is licensed under a Creative Commons Attribution 4.0 International License.
Read Full License

**Additional Declarations:** No competing interests reported.

# Abstract

To explore associations between cortical morphology and cognitive impairment in end-stage kidney disease patients with mild cognitive impairment (ESKD-MCI) and characterized topological alterations of their structural covariance network (SCN) to elucidate underlying neural injury mechanisms. The study enrolled 89 ESKD-MCI patients and 100 healthy controls (HCs). All participants underwent high-resolution T1-weighted MRI and Montreal Cognitive Assessment (MoCA); ESKD-MCI patients also provided blood samples. Surface-based morphometry (SBM) using CAT12 quantified cortical thickness, cortical complexity, sulcal depth, and gyrification index. We tested correlations among cortical metrics, MoCA scores, and blood parameters, and constructed SCNs for groupwise graph-theory comparison. Relative to HCs, ESKD-MCI patients exhibited impaired global cognition and deficits across multiple cognitive subdomains. Neuroanatomically, they showed widespread reductions in cortical thickness, cortical complexity, and gyrification, together with focal increases in sulcal depth, most prominently in the rostral middle frontal gyrus (rMFG). Cortical complexity in the right rMFG correlated positively with MoCA total score ($P$ = 0.013, FWE-corrected). Serum phosphorus correlated negatively with MoCA total score (r = -0.226, $P$ = 0.033). Graph-theory analysis of the SCN revealed decreased whole-brain clustering coefficient and reduced local efficiency in patients, with no significant nodal-level differences. These findings indicate that abnormal cortical morphology and diminished local network efficiency may contribute to cognitive impairment in ESKD-MCI. The negative association between serum phosphorus and cognitive performance suggests that elevated phosphorus is a potential modifiable risk factor and warrants clinical monitoring and control.


# Introduction

End-stage kidney disease (ESKD), the terminal stage of chronic kidney disease (CKD), necessitates life-sustaining renal replacement therapies such as hemodialysis, peritoneal dialysis, or kidney transplantation. Patients with ESKD are at markedly increased risk for cognitive impairment; prevalence estimates reach as high as 87% among those receiving hemodialysis (C. K. Liu et al., 2025). Cognitive deficits in ESKD span multiple domains and contribute to reduced quality of life, functional decline, and worse clinical outcomes (Chan et al., 2023; Viggiano, Wagner, Martino, et al., 2020). Mild cognitive impairment (MCI), an intermediate state between normal cognitive aging and dementia, occurs 2–3 times more often in ESKD patients than in age-matched community populations (Viggiano, Wagner, Blankestijn, et al., 2020). Because 5% to 10% of individuals with MCI progress to clinical dementia (Manly et al., 2008), elucidating the neuropathological mechanisms of MCI in ESKD is essential for early detection and interventions that may prevent irreversible decline.

A prevailing theory attributes cognitive impairment in ESKD to vascular injury, accumulation of uremic toxins, neurotoxicity, neuroinflammation, and oxidative stress (Ikram, 2025). These mechanisms are interrelated and form a complex pathological network. To map the causal chain from molecular disturbances to clinical cognitive phenotypes, biomarkers that link molecular changes to neural and behavioral outcomes are urgently needed. Quantitative structural magnetic resonance imaging (MRI)

provides a noninvasive, radiation-free, and objective research tool for probing relationships between complex behavioral phenotypes (e.g., dementia and MCI) and putative molecular drivers (e.g., uremic toxins) in ESKD, thereby helping to clarify the neural mechanisms of cognitive impairment in this population.

Structural MRI studies of gray matter in ESKD have largely targeted volume and cortical thickness using voxel-based morphometry (VBM) and surface-based morphometry (SBM). These investigations report morphological alterations in regions supporting higher-order cognition—most consistently the prefrontal cortex, hippocampus, and thalamus—and link such changes to cognitive impairment and accumulation of uremic metabolites (Dong et al., 2018; Fang et al., 2024; Gu et al., 2021; Y. Liu et al., 2024; H. Wang et al., 2022; Yuan et al., 2022) However, heterogeneous cohorts, divergent methodologies, and small sample sizes have produced inconsistent results, so a definitive morphological signature for ESKD-MCI remains unresolved. SBM, a high-fidelity structural MRI approach, quantifies cortical thickness, cortical complexity (i.e. fractal dimension), and other surface metrics to detect subtle gray-matter alterations (Ghosh et al., 2022). By aligning brains along the pial surface rather than volumetric voxels, SBM reduces sulcal-pattern misregistration, limits atlas-dependent false positives, and resolves submillimeter abnormalities, thereby providing multidimensional pathological fingerprints (Ghosh et al., 2022; Takao et al., 2022). These features have advanced SBM to the forefront of research on cognitive impairment, from MCI to Alzheimer's disease (AD). Complementing regional morphometry, structural covariance networks (SCNs) measure interregional morphological correlations that reflect coordinated development or shared pathology (Alexander-Bloch et al., 2013; S. Li et al., 2022) Applied with graph-theoretical analysis, SCNs have characterized network efficiency and topological disruption in neuropsychiatric conditions, including AD (Pelkmans et al., 2021). In prodromal AD marked by MCI, SCN abnormalities associate with beta-amyloid (Aβ) and tau pathology. For example, tau deposition reduces small-world properties and global efficiency, indicating early network disintegration (Pelkmans et al., 2021). Thus, SCNs could serve as biomarkers to track disease progression in MCI and to dissect compensatory mechanisms. However, to our knowledge, studies that specifically target the ESKD-MCI population remain scarce.

In this study, we applied the SBM method to compare cortical thickness, cortical complexity, sulcus depth, and local gyrification index in ESKD-MCI patients undergoing hemodialysis. We then examined correlations between these cortical morphological changes and patients' cognitive performance and clinical hematological indicators. Finally, we constructed the topological features of SCNs in ESKD-MCI patients using graph theory analyses to further clarify the underlying neurobiological mechanisms.

## Materials and Methods

# Participants

This study is a clinical trial. The protocol was registered with ClinicalTrials.gov (NCT03961724) on May 23, 2019, by the First Affiliated Hospital of Xi'an Jiaotong University, and approved by the local ethics committee (XJTU1AF-CRF-2018-006). Between April 2019 and May 2024, we recruited 99 patients with

ESKD receiving maintenance hemodialysis who also had mild cognitive impairment (ESKD-MCI) from the nephrology departments of local hospitals. Imaging data from 10 patients were excluded because head motion introduced artifacts on MRI scans, leaving 89 patients for statistical analysis. Additionally, we recruited 100 HCs through local community advertisements; these controls had no history of neurological, psychiatric, or other major medical conditions and all had a MoCA score ≥ 26.

## Inclusion and exclusion criteria

Inclusion criteria for the patient group were: (1) age 18–65 years; (2) estimated glomerular filtration rate (eGFR) < 15 mL/min/1.73 m² and receiving regular maintenance hemodialysis for at least 3 months; (3) primary diagnosis of chronic glomerulonephritis or renal interstitial disease; (4) no prior kidney transplantation; and (5) mild cognitive impairment (MCI) according to the 2003 International Working Group, defined as a Montreal Cognitive Assessment (MoCA) score ≥ 18 and < 26 (Winblad et al., 2004).

Exclusion criteria were: (1) history of psychiatric or neurological disorders, organic brain disease, or diabetes; (2) history of substance abuse or alcohol dependence; (3) visually apparent significant T2 brain lesions on MRI; (4) previously diagnosed dementia, including Alzheimer's disease, frontotemporal dementia, or Parkinson's disease dementia; (5) MoCA score < 18 or ≥ 26; (6) contraindications to MRI; and (7) inability to cooperate with MRI or cognitive assessments.

## Cognitive function assessment and blood biochemical examination

All participants completed standardized cognitive assessments before MRI. Global cognition was measured using the Beijing version of the Montreal Cognitive Assessment (MoCA), which evaluates visuospatial/executive function, naming, attention, language, abstraction, delayed recall, and orientation (Nasreddine et al., 2005).

For all patients with ESKD-MCI, blood biochemical tests were obtained 24 hours before MRI and included hemoglobin (g/L), blood urea nitrogen (BUN, mmol/L), serum creatinine (SCr, μmol/L), calcium (mmol/L), phosphorus (mmol/L), potassium (mmol/L), and parathyroid hormone (PTH, pg/mL).

## MRI Data Acquisition

All MRI scans were performed on a 3 Tesla GE Excite scanner (GE Medical Systems, Milwaukee, WI, USA) equipped with an 8-channel head coil. Subjects also underwent T2-weighted and T2-weighted fluid-attenuated inversion recovery sequences to exclude brain lesions or other abnormalities. Structural images were acquired with a T1-weighted three-dimensional fast spoiled gradient echo sequence using the following parameters: 140 axial slices; slice thickness = 1.0 mm; echo time = 4.8 ms; repetition time = 10.8 ms; flip angle = 9°; no gap; matrix = 256 × 256; field of view = 256 × 256 mm².

## Image data processing

We processed structural images with the Computational Anatomy Toolbox 12 (CAT12, http://www.neuro.uni-jena.de/cat/), an extension of Statistical Parametric Mapping 12 (SPM12, http://www.fil.ion.ucl.ac.uk/spm/software/spm12/) running in MATLAB 2021a (MathWorks Inc., Natick, USA). Following the standard protocol (http://www.neuro.uni-jena.de/cat12/CAT12-Manual.pdf), we performed SBM using the toolbox defaults. The preprocessing pipeline comprised tissue segmentation, spatial registration, surface reconstruction, and surface registration. Participants with image-quality ratings of E or below were excluded after preprocessing. Finally, we smoothed and resampled cortical thickness with a 15 mm full-width-at-half-maximum (FWHM) kernel, while cortical complexity, sulcus depth, and the local gyrification index were smoothed with a 20 mm FWHM kernel.

# Structural covariance network construction

Using MATLAB and a 246-region brain-network atlas (Fan et al., 2016), we extracted SBM parameters for both groups. We treated each region as a network node and constructed a partial-correlation covariance matrix in which the correlation coefficient served as the edge weight. After regressing out covariates (sex, age, education, and total intracranial volume), we computed topological metrics of the structural covariance networks. To ensure full connectedness, we thresholded networks across a sparsity range of 0.03–0.37 (step size = 0.01), excluding any thresholds that produced isolated nodes. We verified the non-randomness of the topology by 2,000 permutations and by comparison with 200 degree-matched random graphs. For each threshold, we summarized global properties (characteristic path length, clustering coefficient, global efficiency, local efficiency, small-world) and nodal properties (betweenness centrality, degree, efficiency) of the SCN using the area under the curve (AUC).

# Statistical analysis

Statistical analyses were conducted with SPSS (version 26.0; IBM Corp., Armonk, NY, USA). Normality was assessed by the Shapiro–Wilk test, and homogeneity of variance by Levene's test. Normally distributed data are reported as mean ± standard deviation; non-normally distributed data are reported as median (interquartile range).

Group differences in demographic and clinical variables were evaluated as follows. Quantitative variables that met normality and variance equality were compared with independent two-sample *t*-tests. Quantitative variables that did not meet normality were compared with the Mann–Whitney *U* test. Categorical variables were compared with the chi-square test.

For voxel-wise analyses, two-sample *t*-tests were performed in the second-level general linear model of SPM12, specifying two groups and including age, sex, and education as covariates. Statistical maps were thresholded at an uncorrected voxel-wise $P < 0.001$ and then subjected to family-wise error (FWE) correction at $P < 0.05$, using the DK40 brain template. Results were visualized with CAT12.

Associations between cortical morphological metrics and clinical variables were tested using multiple regression within the second-level general linear model of SPM12. Correlations between MoCA scores and clinical blood parameters were examined in SPSS, using Pearson's correlation for normally distributed variables and Spearman's correlation for non-normally distributed variables. A *P*-value < 0.05 was considered statistically significant.

## Results

# Demographic and clinical characteristics

A total of 89 ESKD-MCI patients and 100 HCs were included in this study (Fig. 1). Table 1 summarizes group differences in demographic and clinical characteristics. The groups did not differ significantly by sex, age, or education level. The ESKD-MCI group had a lower body mass index (BMI) than HCs and exhibited worse global cognition and deficits across multiple cognitive domains ($P < 0.001$). In clinical blood tests, the ESKD-MCI group showed lower mean hemoglobin and calcium levels, while mean BUN, creatinine, phosphorus, and PTH levels were significantly higher.

Table 1
Demographic information and clinical characteristics in patients with ESKD and HCs.

| **Variables** | **HCs (n = 100)** | **ESKD-MCI (n = 89)** | $\chi^2$ / *U* | ***P*-value** |
|---|---|---|---|---|
| Sex (F / M) | 45 / 55 | 33 / 56 | 1.22[a] | 0.270 |
| Age (years) | 42.00 (26.00) | 41.58 ± 11.25 | 4359.50[b] | 0.809 |
| Education (years) | 12.00 (2.00) | 12.00 (4.00) | 5145.50[b] | 0.060 |
| BMI | 23.17 (4.42) | 21.58 ± 3.36 | 5818.50[b] | **< 0.001** |
| Duration (months) | / | 34.00 (43.00) | / | / |
| MoCA | 29.00 (3.00) | 23.00 (3.00) | 8894.50[b] | **< 0.001** |
| V/E | 5.00 (1.00) | 3.00 (2.00) | 7844.50[b] | **< 0.001** |
| N | 3.00 (0) | 2.00 (1.00) | 6811.50[b] | **< 0.001** |
| A | 6.00 (0) | 5.00 (2.00) | 7030.00[b] | **< 0.001** |
| L | 3.00 (1.00) | 2.00 (1.00) | 6319.50[b] | **< 0.001** |
| Abs | 2.00 (0) | 1.00 (1.00) | 6902.50[b] | **< 0.001** |
| DR | 4.00 (1.00) | 3.00 (1.00) | 7354.00[b] | **< 0.001** |
| O | 6.00 (0) | 6.00 (1.00) | 5772.00[b] | **< 0.001** |
| Hemoglobin (g/L) | NA | 107.31 ± 20.85 | / | / |
| BUN (mmol/L) | NA | 21.76 ± 7.03 | / | / |
| Creatinine (μmol/L) | NA | 903.39 ± 230.09 | / | / |
| Calcium (mmol/L) | NA | 2.14 (0.32) | / | / |
| Phosphorus (mmol/L) | NA | 1.86 ± 0.58 | / | / |
| Potassium (mmol/L) | NA | 4.70 ± 1.03 | / | / |
| PTH (pg/ml) | NA | 418.00 (525.44) | / | / |

Sex is reported as frequencies. Mean ± standard deviation is reported. Medians and interquartile ranges are reported. [a]Analyzed using chi-square test; [b]Analyzed using Mann-Whitney *U* test.

ESKD-MCI: end-stage kidney disease patients with mild cognitive impairment; HCs: health controls; BMI: body mass index; MoCA: Montreal cognitive assessment; V/E: visuospatial/executive; N: naming; A: attention; L: language; Abs: abstraction; DR: delayed recall; O: orientation; BUN: blood urea nitrogen; PTH: parathyroid hormone.

# Group differences in cortical thickness, cortical complexity, sulcal depth, and local gyrification index

The cortical thickness of the ESKD-MCI group was significantly lower than that of HCs across extensive bilateral frontal regions (middle frontal, superior frontal, orbitofrontal, inferior frontal, frontal pole, precentral gyrus, anterior cingulate gyrus, and posterior cingulate gyrus), in portions of the bilateral occipital cortex (pericalcarine and cuneus), in parts of the left temporal lobe (supramarginal gyrus, superior temporal gyrus, transverse temporal gyrus, bankssts [banks of the superior temporal sulcus]), in sections of the left parietal lobe (postcentral gyrus and inferior parietal gyrus), and in the right lateral occipital gyrus. No regions showed significantly increased cortical thickness in ESKD-MCI relative to HCs.

Fractal dimension was significantly lower in ESKD-MCI than in HCs in the right rostral middle frontal gyrus (rMFG), the insula, and the superior temporal gyrus. No regions exhibited significantly increased fractal dimension between the two groups.

ESKD-MCI subjects showed greater sulcal depth than HCs across widespread bilateral frontal regions, including the rMFG, medial and lateral orbitofrontal gyri, superior frontal gyrus, pars orbitalis, and frontal pole. By contrast, ESKD-MCI subjects exhibited reduced sulcal depth relative to HCs in bilateral paracentral lobules, precuneus, and precentral gyri, as well as in the right posterior cingulate gyrus and the left postcentral gyrus, superior parietal gyrus, and insula.

ESKD-MCI subjects also demonstrated a lower local gyrification index than HCs in bilateral supramarginal gyri, insulae, postcentral and precentral gyri, superior and transverse temporal gyri, and the left rMFG. Conversely, the local gyrification index was higher in ESKD-MCI than in HCs in the right postcentral gyrus and paracentral lobule.

These results are illustrated in Fig. 2.

# Correlation of cortical morphological metrics with clinical variables

The fractal dimension of the right rMFG correlated positively with MoCA total score (r = 3.73, $P = 0.013$). MoCA total score correlated negatively with serum phosphorus level (r = -0.226, $P = 0.033$) (see Table 2). However, subsequent mediation analysis did not identify a mediating relationship among these three variables.

Table 2
Correlation between cortical complexity in the right rostral middle frontal gyrus, serum phosphorus level, and MoCA scores.

| Index | FD in right rostral middle frontal gyrus | | MoCA total scores | |
|---|---|---|---|---|
| | ***r* value** | ***p* value** | ***r* value** | ***p* value** |
| MoCA total scores | 3.73 | 0.013 | / | / |
| Phosphorus level | / | / | -0.226 | 0.033 |

FD: fractal dimension; MoCA: Montreal cognitive assessment.

# Intergroup comparisons of SCN

Using the cortical complexity metrics identified in the previous step, we constructed a SCN and compared graph-theoretical measures across groups. Relative to HCs, the ESKD-MCI group showed a lower clustering coefficient ($P = 0.022$) and reduced local efficiency ($P = 0.049$) (Fig. 3). No other network metrics differed significantly between groups.

## Discussion

This study combined SBM with graph theory–based SCN analysis to characterize cortical morphological changes and whole-brain network topology in ESKD-MCI. Compared with HCs, ESKD-MCI patients showed reduced cortical thickness, decreased cortical complexity and local gyrification index, and increased sulcal depth. Cortical complexity in the rostral portion of the right middle frontal gyrus correlated positively with total MoCA scores. Elevated serum phosphorus levels were negatively associated with total MoCA scores. SCN analysis additionally revealed reductions in global clustering coefficient and in local efficiency. Together, these results provide neuroimaging evidence for early neuropathological alterations in ESKD-MCI and implicate hyperphosphatemia as a potential neurotoxic factor affecting brain structure, with implications for clinical strategies such as phosphorus management.

# Cerebral cortical morphological alterations in ESKD-MCI patients

We found that ESKD-MCI patients show widespread cortical thinning, reduced cortical complexity and gyrification index, and increased sulcal depth, concentrated in regions supporting higher cognitive functions: the frontal, temporal, parietal, and occipital lobes. These regions contribute distinctly to cognition: the frontal lobe—especially the prefrontal cortex—supports executive functions, working memory, and attentional regulation (Smucny et al., 2022); the temporal lobe mediates language processing and long-term memory integration (Whitney et al., 2011); the postcentral gyrus together with the inferior parietal lobule converts sensory input into abstract representations used in tasks such as

praxis and digit-symbol substitution (Freedman & Ibos, 2018); and the occipital lobe subserves visual information processing (G. Li et al., 2020). Such diffuse structural alterations likely underlie the multisystem cognitive deficits observed in these patients. Previous studies have documented marked brain atrophy and cognitive decline in ESKD patients following dialysis initiation (Tsuruya & Yoshida, 2024; Zhang et al., 2022). A comparative study of HCs, non-dialysis-dependent CKD patients, and dialysis-dependent CKD patients reported that cortical atrophy in CKD initially affects the frontal, temporal, and occipital lobes and then advances to global brain tissue loss as renal function deteriorates and dialysis dependence emerges (Yu et al., 2023). A Mendelian randomization analysis by Chen et al. established a causal link between kidney impairment and reduced cerebral cortical thickness, with pronounced thinning in frontal and occipital regions (Chen et al., 2021). These reports align with our finding of a trend toward atrophy in the frontal, temporal, parietal, and occipital lobes of ESKD patients. In addition, the reduction in cortical complexity (e.g., in the prefrontal cortex and insula) observed in this study is consistent with the results of our previous study on the decreased cortical complexity in pre-dialysis ESKD patients (Yuan et al., 2022), which further supports the existence of abnormalities in the geometric structure of the brain surface in ESKD patients.

# Relationship between cerebral cortical morphological alterations and cognition

We found a significant positive correlation between cortical complexity in the right rMFG and total MoCA scores ($P = 0.013$). The rMFG occupies the anterior portion of the dorsolateral prefrontal cortex (DLPFC), which serves as a principal node of the DLPFC functional network (Smucny et al., 2022). The DLPFC supports cognitive control, working memory, executive function, and attention regulation (Joyce et al., 2025; Smucny et al., 2022). It integrates multimodal information and suppresses interfering stimuli to sustain goal-directed behavior, and its structural integrity is tightly linked to cognitive flexibility (Joyce et al., 2025). Cortical complexity—measured as fractal dimension in SBM analyses—quantifies the geometric intricacy of the cortical surface. Reduced cortical complexity may reflect simplified dendritic branching, fewer synaptic connections, or abnormal cortical folding (King et al., 2010; Mustafa et al., 2012). Thus, the lower rMFG cortical complexity observed here may signify degenerative changes within DLPFC-related networks and may serve as a neural marker of cognitive impairment in ESKD-MCI patients.

# Relationship between serum phosphorus levels and cognition

Cognitive decline in ESKD patients results from interacting factors such as vascular injury, systemic inflammation, accumulation of uremic toxins, and metabolic disturbances. Vascular dysfunction produces small vessel disease and impairs the blood–brain barrier, which can permit substances like BUN, creatinine, and phosphorus to enter the brain and elicit neuroinflammation and oxidative stress that damage neurons and synapses (Rroji et al., 2022; Viggiano, Wagner, Martino, et al., 2020). Dialysis removes some metabolic wastes, but aspects of hemodialysis—intermittent fluid removal, hemodynamic

stress, solute clearance, disruption of sodium homeostasis, and proinflammatory stimuli—increase the risk of acute brain injury and, over time, cumulative chronic damage when vascular regulatory mechanisms are compromised. These processes together promote the progressive cognitive decline observed in ESKD (McIntyre & Jain, 2025).

In this study, ESKD-MCI patients had higher serum phosphorus levels that correlated negatively with total MoCA scores (r = -0.226, *P* = 0.033), indicating that hyperphosphatemia may contribute to cognitive impairment. In ESKD, a marked decline in glomerular filtration rate impairs renal phosphate excretion. Although compensatory rises in PTH and fibroblast growth factor 23 (FGF23) initially promote urinary phosphate loss by inhibiting tubular phosphate reabsorption (for example, via downregulation of NaPi-IIa/IIc transporters), these mechanisms fail as renal function worsens (Rroji et al., 2022). At the same time, decreased expression of klotho, the FGF23 co-receptor, reduces FGF23 bioactivity and favors phosphate retention, producing hyperphosphatemia (Rroji et al., 2022).

Elevated serum phosphate promotes endothelial dysfunction by inhibiting endothelial nitric oxide synthase and fostering vascular calcification, particularly within cerebral small vessels; these changes impair cerebral perfusion and contribute to white matter lesions and microinfarcts (Chung et al., 2019). Serum phosphate also induces proinflammatory cytokines such as interleukin-1β and tumor necrosis factor-α and increases oxidative stress, which together exacerbate neurovascular injury (Buchanan et al., 2020; Rroji et al., 2022). Beyond vascular effects, phosphate toxicity can directly damage neurons through mitochondrial dysfunction, tau hyperphosphorylation that favors neurofibrillary tangle formation, and enhanced apoptotic pathways (Chen et al., 2022; Rroji et al., 2022). A cohort of 744,235 U.S. veterans showed that elevated serum phosphate independently increased the risk of developing dementia, with the effect being stronger in individuals younger than 60 years (T. Li et al., 2017). In patients with CKD stages 3–5, MoCA scores were inversely correlated with serum phosphate levels (Aggarwal et al., 2020). These observations align with our findings and support more rigorous monitoring and management of serum phosphorus in patients with ESKD.

# Impaired global topological organization of SCNs in ESKD-MCI patients

SCNs quantify covariance relationships in morphological features, such as cortical thickness and cortical complexity, across brain regions, thereby reflecting coordinated patterns of change during neurodevelopment or neurodegeneration. By operating at the whole-brain level rather than relying on predefined regions, SCN construction captures dynamic structural reorganization that region-based approaches may miss (Arslan et al., 2018). In this study, we built SCNs from cortical complexity and applied graph-theory analyses; compared with HCs, ESKD-MCI patients showed significantly reduced global clustering coefficient and local efficiency. The clustering coefficient indexes connection density within local neighborhoods and thus reflects the degree of functional modularization, while local efficiency measures information-transfer efficiency among neighboring nodes and relates closely to network robustness against perturbations (Latora & Marchiori, 2001; Rubinov & Sporns, 2010). The

observed reductions in these metrics therefore indicate impaired global modular integration and decreased local information-transfer efficiency in ESKD-MCI. Notably, nodal metrics did not differ significantly, suggesting that the pathological process in ESKD-MCI preferentially alters global topology rather than targeting specific brain regions. This pattern mirrors early SCN alterations reported in neurodegenerative disorders such as AD, where abnormalities in global network efficiency precede regional atrophy (Mongay-Ochoa et al., 2025; Voevodskaya et al., 2018). Prior studies also reported impairments in gray matter and functional networks in ESKD patients (Y. Wang et al., 2024; Zheng et al., 2022), which aligns with our findings. Focusing on the earlier, more clinically actionable stage of ESKD-MCI, this study is the first to apply SCN analysis based on cortical complexity and thus offers a novel structural-network perspective on the neural mechanisms underlying ESKD-MCI.

This study has several limitations. First, its cross-sectional design prevents definitive conclusions about the causal link between cortical morphological changes and cognitive impairment. Future research should use multi-center longitudinal cohorts to follow ESKD patients as they progress from cognitively normal status to MCI. Second, because we did not include an ESKD control group without MCI, we cannot distinguish alterations specific to MCI from those associated with ESKD itself. Third, the absence of multimodal brain imaging limits mechanistic insight; future studies should combine other examination methods, and molecular biomarkers to clarify how structural damage, cerebral blood flow, and functional network disturbances interact and to identify objective, stable neuroimaging markers for early screening of ESKD-related MCI.

## Conclusions

This study identified widespread cortical morphological abnormalities in ESKD-MCI patients. Reduced cortical complexity in the right rMFG, together with disrupted global network modular integration and diminished local information-transfer efficiency, likely constitute central neural mechanisms underlying brain injury in ESKD-MCI. Moreover, elevated serum phosphorus emerged as a potential risk factor, highlighting the clinical importance of rigorous monitoring and management of phosphorus levels.

## Declarations

# Competing Interests

The authors have no relevant financial or non-financial interests to disclose.

### Ethics approval

This study was approved by ethics committee of the First Affiliated Hospital of Xi’an Jiaotong University (ID: XJTU1AF2018LSL-006). Written informed consent was obtained in accordance with the Declaration of Helsinki (1964) from each patient or their guardians.

**Consent to participate**

Informed consent was obtained from all individual participants included in the study.

**Consent for publication**

Not applicable.

# Funding

This study was supported by the Health Research and Innovation Capacity Strengthening Platform Program of Shaanxi Province (Grant Number 2023PT-09), the Clinical Research Award of the First Affiliated Hospital of Xi'an Jiaotong University (Grant Number XJTU1AF-CRF-2023–021), the Key Research and Development Plan of Xianyang City ((Grant No. L2023-ZDYF-SF-035 and L2022ZDYF-SF-026), and the Science and Technology Research Project of Shaanxi Nuclear Industry Group Co. Ltd. (Grant No. 61240302).

# Author Contribution

All authors contributed to the study conception and design. Material preparation was performed by Jing Yang, Huijie Yuan, Junya Mu, and Ming Zhang. Analysis was performed by Jing Yang, Huijie Yuan, Xia Luo, Zhaoyao Luo, and Qiange Zhu. Data collection was performed by Xia Luo, Zhaoyao Luo, Wen Gu, Shaohui Ma, Peng Li, Dun Ding, and Xueying Ma. The first draft of the manuscript was written by Jing Yang and Huijie Yuan, and all authors commented on previous versions of the manuscript. All authors read and approved the final manuscript.

# Acknowledgement

We thank the all participants and staff involved in this study.

# Data Availability

The datasets generated during and/or analysed during the current study are not publicly available due to the inclusion of sensitive clinical information and individual participant privacy protection requirements, but are available from the corresponding author on reasonable request.

## References

1. Aggarwal, H. K., Jain, D., & Bhavikatti, A. (2020). Cognitive Dysfunction in Patients with Chronic Kidney Disease. *Saudi J Kidney Dis Transpl*, *31*(4), 796–804. https://doi.org/10.4103/1319-

2442.292313

2. Alexander-Bloch, A., Giedd, J. N., & Bullmore, E. (2013). Imaging structural co-variance between human brain regions. *Nature Reviews Neuroscience*, *14*(5), 322–336. https://doi.org/10.1038/nrn3465
3. Arslan, S., Ktena, S. I., Makropoulos, A., Robinson, E. C., Rueckert, D., & Parisot, S. (2018). Human brain mapping: A systematic comparison of parcellation methods for the human cerebral cortex. *Neuroimage*, *170*, 5–30. https://doi.org/10.1016/j.neuroimage.2017.04.014
4. Buchanan, S., Combet, E., Stenvinkel, P., & Shiels, P. G. (2020). Klotho, Aging, and the Failing Kidney. *Front Endocrinol (Lausanne)*, *11*, 560. https://doi.org/10.3389/fendo.2020.00560
5. Chan, F. H. F., Goh, Z. Z. S., Zhu, X., Car, T., Newman, L., Khan, S., B. A., & Griva, K. (2023). Subjective cognitive complaints in end-stage renal disease: a systematic review and meta-analysis. *Health Psychol Rev*, *17*(4), 614–640. https://doi.org/10.1080/17437199.2022.2132980
6. Chen, X., Chen, L., Lin, G., Wang, Z., Kodali, M. C., Li, M., Chen, H., Lebovitz, S. G., Ortyl, T. C., Li, L., Ismael, S., Singh, P., Malik, K. U., Ishrat, T., Zhou, F. M., Zheng, W., & Liao, F. F. (2022). White matter damage as a consequence of vascular dysfunction in a spontaneous mouse model of chronic mild chronic hypoperfusion with eNOS deficiency. *Molecular Psychiatry*, *27*(11), 4754–4769. https://doi.org/10.1038/s41380-022-01701-9
7. Chen, X., Kong, J., Pan, J., Huang, K., Zhou, W., Diao, X., Cai, J., Zheng, J., Yang, X., Xie, W., Yu, H., Li, J., Pei, L., Dong, W., Qin, H., Huang, J., & Lin, T. (2021). Kidney damage causally affects the brain cortical structure: A Mendelian randomization study. *EBioMedicine*, *72*, 103592. https://doi.org/10.1016/j.ebiom.2021.103592
8. Chung, C. P., Peng, L. N., Chou, K. H., Liu, L. K., Lee, W. J., Lin, C. P., Chen, L. K., & Wang, P. N. (2019). High Circulatory Phosphate Level Is Associated with Cerebral Small-Vessel Diseases. *Transl Stroke Res*, *10*(3), 265–272. https://doi.org/10.1007/s12975-018-0639-6
9. Dong, J., Ma, X., Lin, W., Liu, M., Fu, S., Yang, L., & Jiang, G. (2018). Aberrant cortical thickness in neurologically asymptomatic patients with end-stage renal disease. *Neuropsychiatric Disease And Treatment*, *14*, 1929–1939. https://doi.org/10.2147/ndt.S170106
10. Fan, L., Li, H., Zhuo, J., Zhang, Y., Wang, J., Chen, L., Yang, Z., Chu, C., Xie, S., Laird, A. R., Fox, P. T., Eickhoff, S. B., Yu, C., & Jiang, T. (2016). The Human Brainnetome Atlas: A New Brain Atlas Based on Connectional Architecture. *Cerebral Cortex*, *26*(8), 3508–3526. https://doi.org/10.1093/cercor/bhw157
11. Fang, J., Xu, H., Zhou, Y., Zou, F., Zuo, J., Wu, J., Wu, Q., Qi, X., & Wang, H. (2024). Altered brain texture features in end-stage renal disease patients: a voxel-based 3D brain texture analysis study. *Front Neurosci*, *18*, 1471286. https://doi.org/10.3389/fnins.2024.1471286
12. Freedman, D. J., & Ibos, G. (2018). An Integrative Framework for Sensory, Motor, and Cognitive Functions of the Posterior Parietal Cortex. *Neuron*, *97*(6), 1219–1234. https://doi.org/10.1016/j.neuron.2018.01.044

13. Ghosh, A., Kaur, S., Shah, R., Oomer, F., Avasthi, A., Ahuja, C. K., Basu, D., Nehra, R., & Khandelwal, N. (2022). Surface-based brain morphometry in schizophrenia vs. cannabis-induced psychosis: A controlled comparison. *Journal Of Psychiatric Research*, *155*, 286–294. https://doi.org/10.1016/j.jpsychires.2022.09.034
14. Gu, W., He, R., Su, H., Ren, Z., Zhang, L., Yuan, H., Zhang, M., & Ma, S. (2021). Changes in the Shape and Volume of Subcortical Structures in Patients With End-Stage Renal Disease. *Frontiers In Human Neuroscience*, *15*, 778807. https://doi.org/10.3389/fnhum.2021.778807
15. Ikram, M. A. (2025). Chronic kidney disease and dementia: an epidemiological perspective. *Nature Reviews Nephrology*, *21*(8), 525–535. https://doi.org/10.1038/s41581-025-00967-w
16. Joyce, M. K. P., Uchendu, S., & Arnsten, A. F. T. (2025). Stress and Inflammation Target Dorsolateral Prefrontal Cortex Function: Neural Mechanisms Underlying Weakened Cognitive Control. *Biological Psychiatry*, *97*(4), 359–371. https://doi.org/10.1016/j.biopsych.2024.06.016
17. King, R. D., Brown, B., Hwang, M., Jeon, T., & George, A. T. (2010). Fractal dimension analysis of the cortical ribbon in mild Alzheimer's disease. *Neuroimage*, *53*(2), 471–479. https://doi.org/10.1016/j.neuroimage.2010.06.050
18. Latora, V., & Marchiori, M. (2001). Efficient behavior of small-world networks. *Physical Review Letters*, *87*(19), 198701. https://doi.org/10.1103/PhysRevLett.87.198701
19. Li, G., Huang, S., Xu, W., Jiao, W., Jiang, Y., Gao, Z., & Zhang, J. (2020). The impact of mental fatigue on brain activity: a comparative study both in resting state and task state using EEG. *Bmc Neuroscience*, *21*(1), 20. https://doi.org/10.1186/s12868-020-00569-1
20. Li, S., Bai, R., Yang, Y., Zhao, R., Upreti, B., Wang, X., Liu, S., Cheng, Y., & Xu, J. (2022). Abnormal cortical thickness and structural covariance networks in systemic lupus erythematosus patients without major neuropsychiatric manifestations. *Arthritis Res Ther*, *24*(1), 259. https://doi.org/10.1186/s13075-022-02954-z
21. Li, T., Xie, Y., Bowe, B., Xian, H., & Al-Aly, Z. (2017). Serum phosphorus levels and risk of incident dementia. *PLoS One*, *12*(2), e0171377. https://doi.org/10.1371/journal.pone.0171377
22. Liu, C. K., Cheung, K. L., & Tamura, M. K. (2025). Diagnosis and Management of Dementia for the Nephrology Clinician: A Review. *American Journal Of Kidney Diseases*, *86*(1), 97–108. https://doi.org/10.1053/j.ajkd.2025.01.007
23. Liu, Y., Wang, H., Sha, G., Cao, Y., Chen, Y., Chen, Y., Zhang, J., Chai, C., Fan, Q., & Xia, S. (2024). The covariant structural and functional neuro-correlates of cognitive impairments in patients with end-stage renal diseases. *Front Neurosci*, *18*, 1374948. https://doi.org/10.3389/fnins.2024.1374948
24. Manly, J. J., Tang, M. X., Schupf, N., Stern, Y., Vonsattel, J. P., & Mayeux, R. (2008). Frequency and course of mild cognitive impairment in a multiethnic community. *Annals Of Neurology*, *63*(4), 494–506. https://doi.org/10.1002/ana.21326
25. McIntyre, C. W., & Jain, A. (2025). Dialysis and cognitive impairment. *Nature Reviews Nephrology*, *21*(8), 553–564. https://doi.org/10.1038/s41581-025-00960-3

26. Mongay-Ochoa, N., Gonzalez-Escamilla, G., Fleischer, V., Pareto, D., Rovira, À., Sastre-Garriga, J., & Groppa, S. (2025). Structural covariance analysis for neurodegenerative and neuroinflammatory brain disorders. *Brain*, *148*(9), 3072–3084. https://doi.org/10.1093/brain/awaf151
27. Mustafa, N., Ahearn, T. S., Waiter, G. D., Murray, A. D., Whalley, L. J., & Staff, R. T. (2012). Brain structural complexity and life course cognitive change. *Neuroimage*, *61*(3), 694–701. https://doi.org/10.1016/j.neuroimage.2012.03.088
28. Nasreddine, Z. S., Phillips, N. A., Bédirian, V., Charbonneau, S., Whitehead, V., Collin, I., Cummings, J. L., & Chertkow, H. (2005). The Montreal Cognitive Assessment, MoCA: a brief screening tool for mild cognitive impairment. *Journal Of The American Geriatrics Society*, *53*(4), 695–699. https://doi.org/10.1111/j.1532-5415.2005.53221.x
29. Pelkmans, W., Ossenkoppele, R., Dicks, E., Strandberg, O., Barkhof, F., Tijms, B. M., Pereira, J. B., & Hansson, O. (2021). Tau-related grey matter network breakdown across the Alzheimer's disease continuum. *Alzheimer'S Research & Therapy*, *13*(1), 138. https://doi.org/10.1186/s13195-021-00876-7
30. Rroji, M., Figurek, A., Viggiano, D., Capasso, G., & Spasovski, G. (2022). Phosphate in the Context of Cognitive Impairment and Other Neurological Disorders Occurrence in Chronic Kidney Disease. *International Journal Of Molecular Sciences*, *23*(13). https://doi.org/10.3390/ijms23137362
31. Rubinov, M., & Sporns, O. (2010). Complex network measures of brain connectivity: uses and interpretations. *Neuroimage*, *52*(3), 1059–1069. https://doi.org/10.1016/j.neuroimage.2009.10.003
32. Smucny, J., Dienel, S. J., Lewis, D. A., & Carter, C. S. (2022). Mechanisms underlying dorsolateral prefrontal cortex contributions to cognitive dysfunction in schizophrenia. *Neuropsychopharmacology : Official Publication Of The American College Of Neuropsychopharmacology*, *47*(1), 292–308. https://doi.org/10.1038/s41386-021-01089-0
33. Takao, H., Amemiya, S., & Abe, O. (2022). Reproducibility of Longitudinal Changes in Cortical Thickness Determined by Surface-Based Morphometry Between Non-Accelerated and Accelerated MR Imaging. *Journal Of Magnetic Resonance Imaging*, *55*(4), 1151–1160. https://doi.org/10.1002/jmri.27929
34. Tsuruya, K., & Yoshida, H. (2024). Cognitive Impairment and Brain Atrophy in Patients with Chronic Kidney Disease. *J Clin Med*, *13*(5). https://doi.org/10.3390/jcm13051401
35. Viggiano, D., Wagner, C. A., Blankestijn, P. J., Bruchfeld, A., Fliser, D., Fouque, D., Frische, S., Gesualdo, L., Gutiérrez, E., Goumenos, D., Hoorn, E. J., Eckardt, K. U., Knauß, S., König, M., Malyszko, J., Massy, Z., Nitsch, D., Pesce, F., Rychlík, I., et al. (2020). Mild cognitive impairment and kidney disease: clinical aspects. *Nephrology, Dialysis, Transplantation*, *35*(1), 10–17. https://doi.org/10.1093/ndt/gfz051
36. Viggiano, D., Wagner, C. A., Martino, G., Nedergaard, M., Zoccali, C., Unwin, R., & Capasso, G. (2020). Mechanisms of cognitive dysfunction in CKD. *Nature Reviews Nephrology*, *16*(8), 452–469. https://doi.org/10.1038/s41581-020-0266-9

37. Voevodskaya, O., Pereira, J. B., Volpe, G., Lindberg, O., Stomrud, E., van Westen, D., Westman, E., & Hansson, O. (2018). Altered structural network organization in cognitively normal individuals with amyloid pathology. *Neurobiology Of Aging*, *64*, 15–24. https://doi.org/10.1016/j.neurobiolaging.2017.11.014
38. Wang, H., Huang, L., Wu, G., Li, J., Liu, L., Zhang, T., Zhu, J., Zhang, X., Shen, W., Chai, C., & Xia, S. (2022). Regional cerebral gray matter atrophy is associated with cognitive impairment in hemodialysis patients: a cross-sectional and longitudinal voxel-based morphological MRI study. *Brain Imaging Behav*, *16*(3), 1284–1293. https://doi.org/10.1007/s11682-021-00602-9
39. Wang, Y., Chen, S., Zhang, P., Zhai, Z., Chen, Z., & Li, Z. (2024). Cortical structural network characteristics in non-cognitive impairment end-stage renal disease. *Front Neurosci*, *18*, 1467791. https://doi.org/10.3389/fnins.2024.1467791
40. Whitney, C., Jefferies, E., & Kircher, T. (2011). Heterogeneity of the left temporal lobe in semantic representation and control: priming multiple versus single meanings of ambiguous words. *Cerebral Cortex*, *21*(4), 831–844. https://doi.org/10.1093/cercor/bhq148
41. Winblad, B., Palmer, K., Kivipelto, M., Jelic, V., Fratiglioni, L., Wahlund, L. O., Nordberg, A., Bäckman, L., Albert, M., Almkvist, O., Arai, H., Basun, H., Blennow, K., de Leon, M., DeCarli, C., Erkinjuntti, T., Giacobini, E., Graff, C., Hardy, J., et al. (2004). Mild cognitive impairment–beyond controversies, towards a consensus: report of the International Working Group on Mild Cognitive Impairment. *Journal Of Internal Medicine*, *256*(3), 240–246. https://doi.org/10.1111/j.1365-2796.2004.01380.x
42. Yu, H., Zhang, C., Cai, Y., Wu, N., Jia, X., Wu, J., Shi, F., Hua, R., & Yang, Q. (2023). Morphological brain alterations in dialysis- and non-dialysis-dependent patients with chronic kidney disease. *Metabolic Brain Disease*, *38*(4), 1311–1321. https://doi.org/10.1007/s11011-022-01150-x
43. Yuan, H., Li, H., Mu, J., Gu, W., Zhu, X., Gao, L., Zhang, Y., & Ma, S. (2022). Reduced cortical complexity in patients with end-stage kidney disease prior to dialysis initiation. *Front Neurosci*, *16*, 971010. https://doi.org/10.3389/fnins.2022.971010
44. Zhang, C., Yu, H., Cai, Y., Wu, N., Liang, S., Zhang, C., Duan, Z., Zhang, Z., & Cai, G. (2022). Diffusion tensor imaging of the brain white matter microstructure in patients with chronic kidney disease and its correlation with cognition. *Frontiers In Neurology*, *13*, 1086772. https://doi.org/10.3389/fneur.2022.1086772
45. Zheng, J., Wu, X., Dai, J., Pan, C., Shi, H., Liu, T., & Jiao, Z. (2022). Aberrant brain gray matter and functional networks topology in end stage renal disease patients undergoing maintenance hemodialysis with cognitive impairment. *Front Neurosci*, *16*, 967760. https://doi.org/10.3389/fnins.2022.967760

# Figures

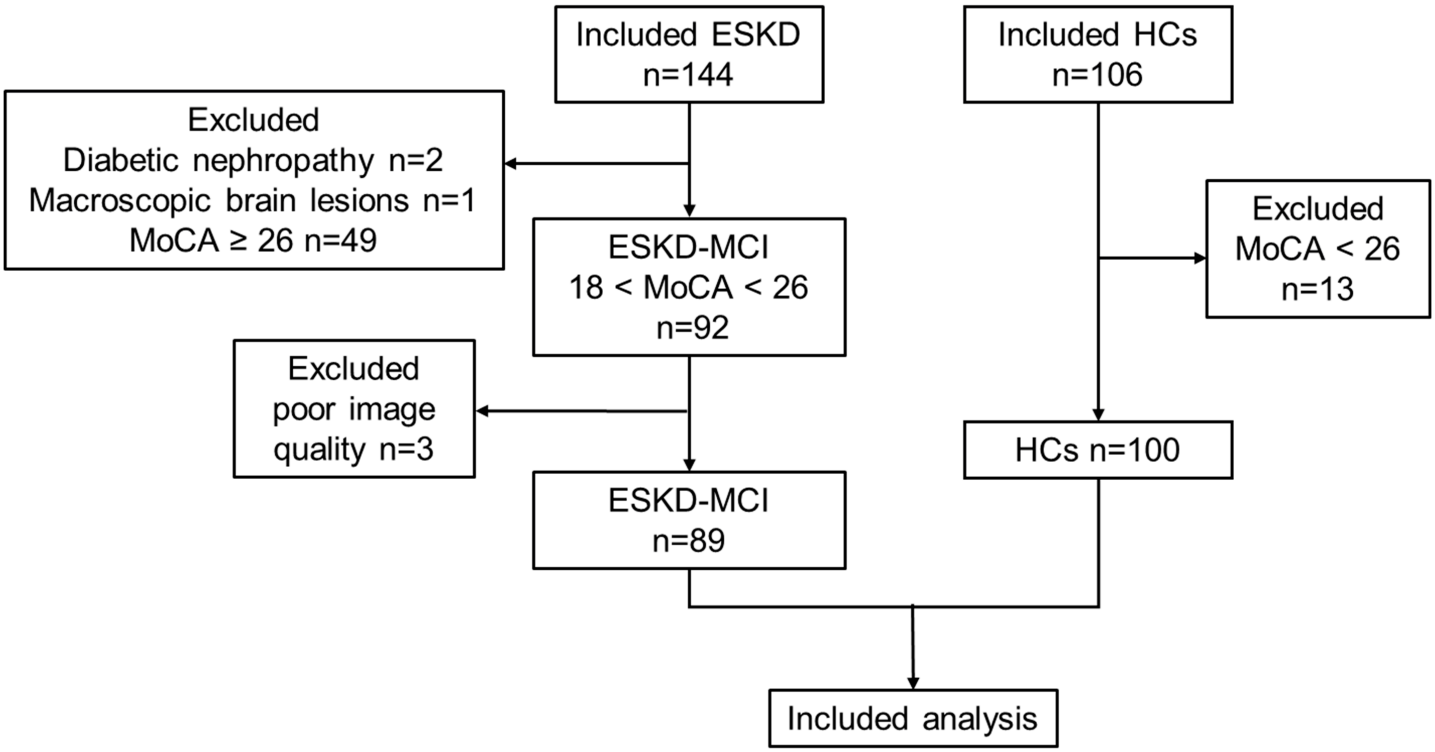



**Figure 1**

The flowchart shows the selection criteria for patients with end-stage kidney disease and mild cognitive impairment (ESKD-MCI) and healthy controls (HCs) in the study. MoCA: Montreal cognitive assessment

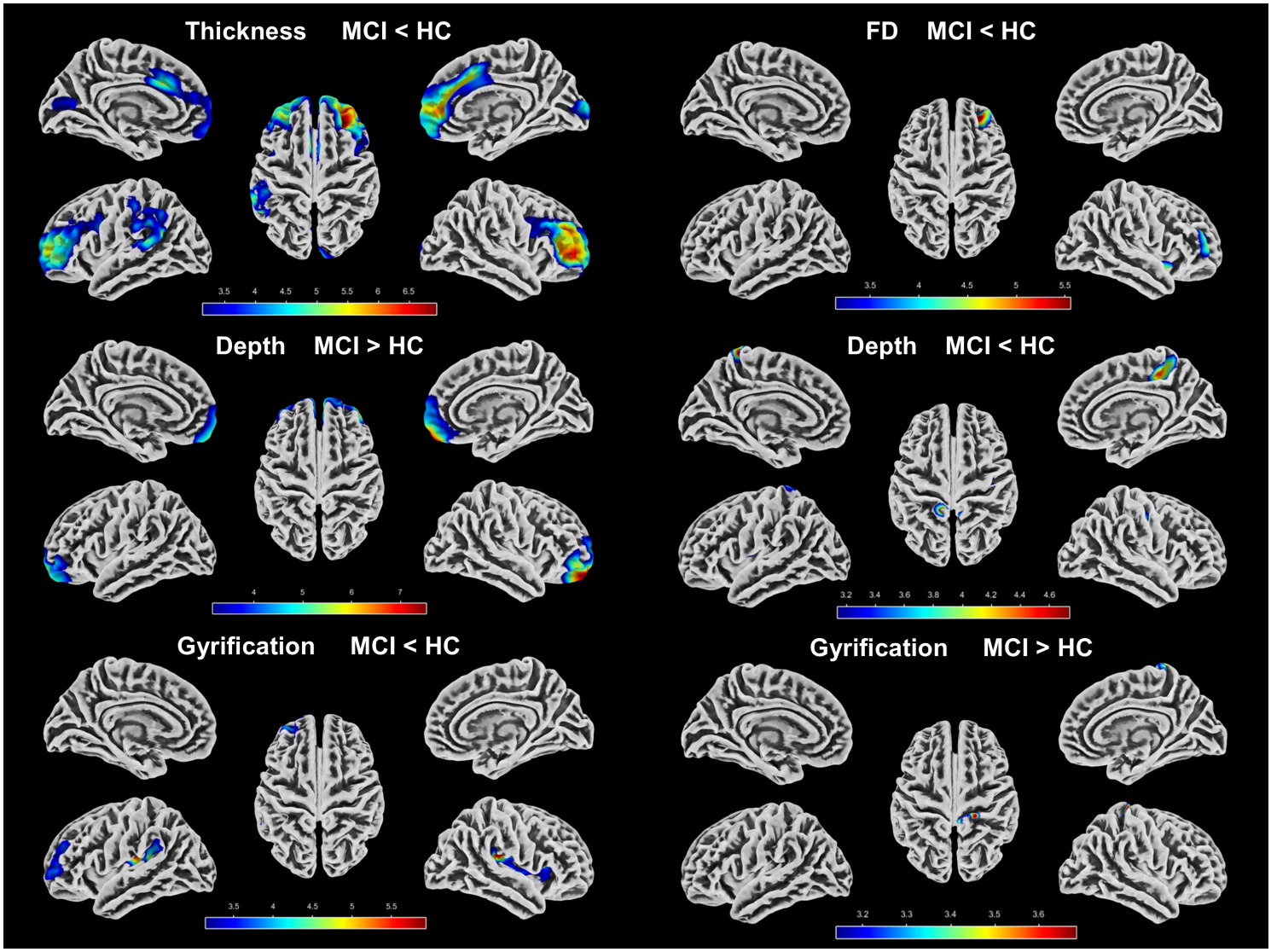



**Figure 2**

Group differences in cortical thickness, fractal dimension (FD), sulcal depth, and cortical gyrification (*P* < 0.05, family-wise error-corrected)

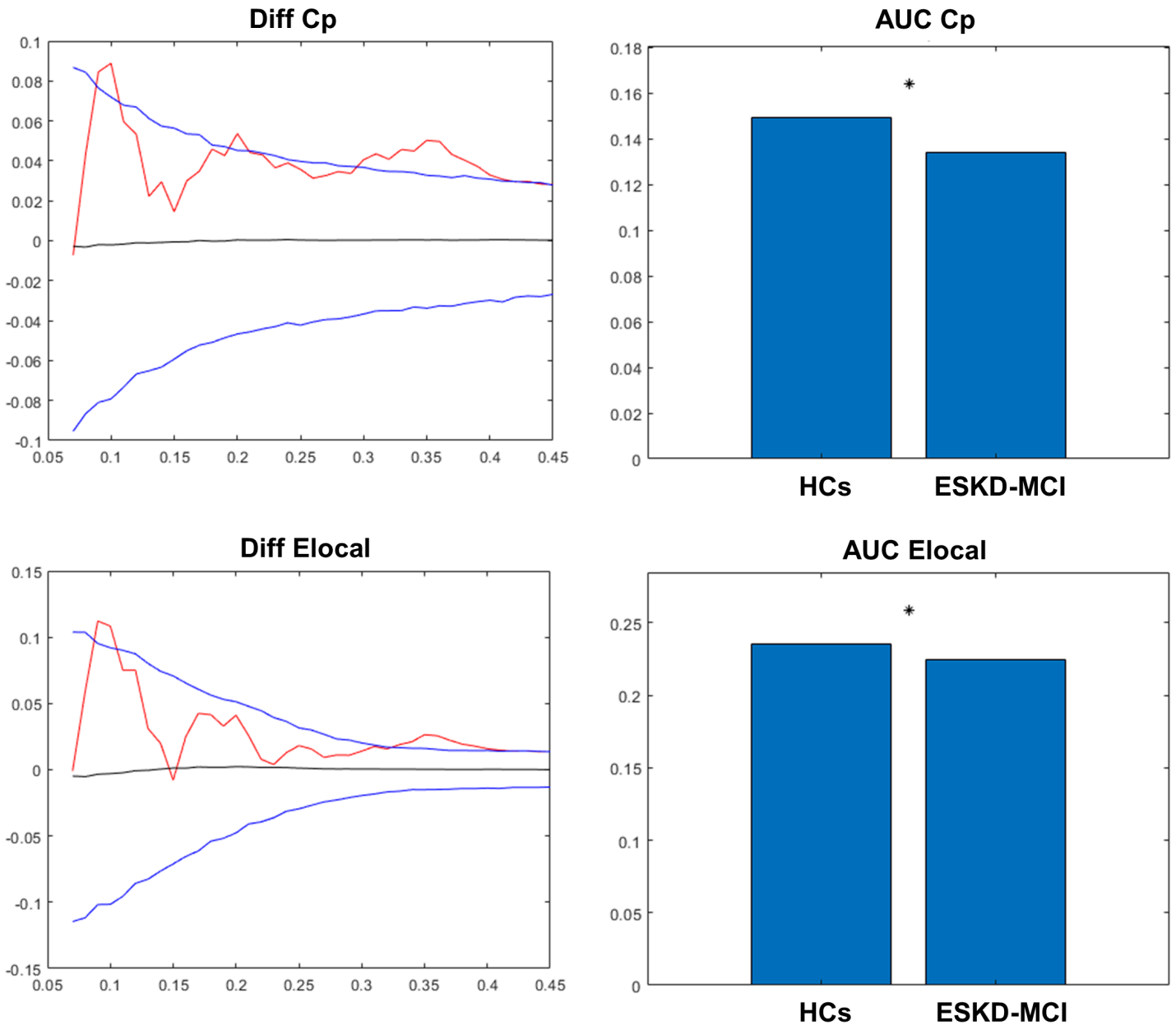



**Figure 3**

Intergroup comparisons of global properties for structural covariance networks (SCN). * *P* < 0.05; Cp: clustering coefficient; Elocal: local efficiency; AUC